A Quantification of the Modelling Uncertainty of Non-linear Finite Element Analyses of Large Concrete Structures

Morten Engen[a,b,*], Max A. N. Hendriks[b,c], Jochen Köhler[b], Jan Arve Øverli[b], Erik Åldstedt[a]

[a] *Multiconsult ASA, Postboks 265 Skøyen, 0213 Oslo, Norway*
[b] *Dept. of Structural Engineering, Norwegian University of Science & Technology, Rich. Birkelandsvei 1A, 7491 Trondheim, Norway*
[c] *Faculty of Civil Engineering & Geosciences, Delft University of Technology, Steinweg 1, 2628CN Delft, The Netherlands*

Abstract

In order to make non-linear finite element analyses applicable during assessment of the global resistance of large concrete structures, there is need for a solution strategy with a low modelling uncertainty. A solution strategy comprises choices regarding force equilibrium, kinematic compatibility and constitutive relations. Relatively large solid finite elements and a fully triaxial material model for concrete were used in the present work. Bayesian inference was applied to results from 38 benchmark analyses. The results indicated that the modelling uncertainty could be represented as a log-normally distributed random variable with mean 1.10 and standard deviation of 0.12. A new method for characterizing the failure mode was developed. The results indicated that the physical uncertainties influenced the estimated parameters of the modelling uncertainty, and that this should be considered when other uncertainties are included in a reliability assessment.

Keywords: Non-linear finite element analyses, Bayesian inference, large concrete shell structures, modelling uncertainty, global resistance, characterization of failure mode

1. Introduction

The design of large concrete shell structures like dams and offshore oil and gas platforms is normally based on global linear finite element analyses. This allows for using the principle of superpositioning in order to handle the vast number of design load combinations [1, 2]. For such large shell structures it is important to perform global analyses due to the interaction between global and local load effects. Solid elements are normally used due to the required accuracy in structural joints, and the elements are large compared to the sectional dimensions.

In order to better take into account the real physical behaviour of reinforced concrete, non-linear finite element analyses (NLFEA) could be carried out. The results of such analyses are global in nature due to all sections contributing to the load carrying capacity [3, 4]. Due to the global nature of NLFEA, the capacity should be assessed in a global manner, in contrast to the local sectional design based on linear finite element analyses. fib *Model Code 2010 for concrete structures* [5] introduces probabilistic methods and the semi-probabilistic concept of global resistance methods for assessing the structural reliability. Demonstrations of the global resistance methods are reported in the literature for relatively simple structural forms [3, 4, 6–12] and also for larger structural systems [13, 14]. For such assessments to be accurate, all relevant sources of uncertainties should be considered. As described by Zhang and Mahadevan [15], there are basically three sources of uncertainties in engineering analyses: *physical uncertainties*, *modelling uncertainties* and *statistical uncertainties*.

In this paper, the different sources of uncertainties are discussed. The modelling uncertainty is further quantified by use of Bayesian inference, and a new method for characterization of the failure mode is presented in order to study the influ-

*Corresponding author
Email address: morten.engen@multiconsult.no (Morten Engen)

ence from the physical uncertainties on the modelling uncertainty. The results indicate that the modelling uncertainty includes contributions from the physical uncertainties, and that this should be considered when other uncertainties are included in a reliability assessment.

2. Uncertainties in engineering analyses

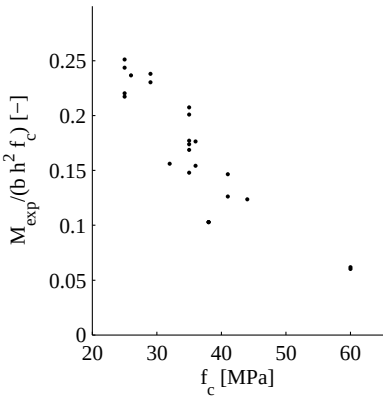

(a) Experimentally obtained moment capacity M_{exp} for ductile beams and walls [20–24] normalized by the width b, height h and cylinder strength f_c plotted against the cylinder strength.

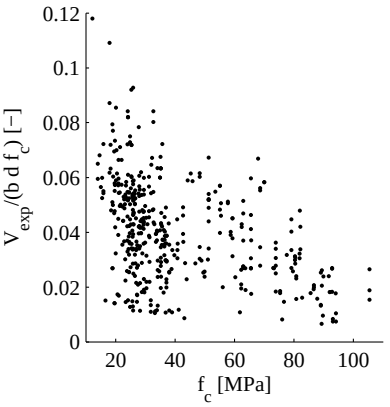

(b) Experimentally obtained shear capacity V_{exp} for brittle beams [25] normalized by the width b, depth d and cylinder strength f_c plotted against the cylinder strength.

Figure 1: Visualization of the physical uncertainty on structural level for a) ductile and b) brittle experiments.

The *physical uncertainties* are related to the measured strength and deformation properties of concrete and reinforcement. The physical uncertainties of concrete and reinforcement on material level is studied by several authors, e.g. Rackwitz [16], and a summary of the results is found in the *Probabilistic Model Code* [17]. The variation of material properties can be studied on several hierarchical levels and can be quantified in terms of the uncertain mean of the gross supply, the variability of the production line of one producer, the variability within one batch and the mean and standard deviation of the material property in a reference volume. By investigation of such results, it can be seen that the variation of the compressive cylinder strength of concrete, denoted by the coefficient of variation, is in the range of 5-15% depending on the cylinder strength, compared to a value of typically 5% for the yield strength of the reinforcement steel. The correlation between the cylinder strength and other properties of concrete is studied by e.g. Rashid et al. [18], where the splitting tensile strength of 499 tested specimens was found to vary within a bandwidth of approximately 30-40% when presented as a function of the compressive cylinder strength.

Ideally, the physical uncertainty on structural level should be assessed by performing a large number of experiments on nominally equivalent components. However, in reality, only a limited amount of results from repeated experiments are reported, and the results are typically normalized in order to assess the physical uncertainty from a range of experiments. The uncertainty found from such a study would also include a contribution from modelling uncertainty due to the selected normalizing factor. Based on the different uncertainties on material level it is expected that the physical uncertainties on structural level depend on whether the failure mode is governed by the concrete or the reinforcement, and expected to be particularly high if the failure mode is governed by the tensile strength of the concrete. This statement is supported in the work of Ellingwood and Galambos [19] where the resistance of reinforced concrete beams failing in bending is found to have a lower coefficient of variation than beams failing in shear. Figure 1a and 1b show normalized results from experiments with ductile [20–24] and brittle [25] failure modes respectively. By investigation of the

variation, the uncertainty of the ductile failure modes is smaller than the uncertainty of the brittle failure modes. A significant *statistical uncertainty* is present in the case of the ductile failure modes due to the limited amount of observations collected in the present study.

Modelling uncertainties, or model uncertainties, in engineering analyses are related to model selection and the accuracy of the selected model, and apply to both statistical and mechanical models. Only the contribution from the accuracy of the mechanical model to the modelling uncertainty was considered in the present work. Models in engineering analyses are never right or wrong, but they can be more or less useful for a certain problem if the modelling uncertainty is appropriately accounted for. The accuracy of the mechanical model depends on the approximations in the numerical solution procedure and the mathematical idealization of the problem. According to Ditlevsen [26] the uncertainties related to the mathematical idealization are due to a limitation of the possible infinite number of basic variables to a finite number and idealizations of the mathematical equations, both for pragmatic reasons and due to a lack of detailed knowledge about the variation or the behaviour of the problem at hand. There are aspects that we know that we do not consider in the model, but also features that we do not know, i.e. the unknown unknowns. The modelling uncertainty thus covers implicitly everything that is not explicitly considered in the model.

The modelling uncertainty can be quantified by *verification* and *validation* [27]. Verification is related to how the equations of the mechanical model are solved, i.e. a quantification of the accuracy without questioning the relation between the equations and the physical problem at hand. With regard to NLFEA, verification thus relates to the iterative solution of the equilibrium equations and the discretization into finite elements. Validation, on the other hand, relates to how well the equations capture the true physical behaviour. In the NLFEA context, validation thus relates to idealization of the geometry and the material behaviour. In other words, verification answers the question *Are we solving the equations right?*, and validation answers the question *Are we solving the right equations?* [27].

This distinction is useful. One cannot expect improved results by refining the element discretization or the iterative solution scheme if the material model is inadequate. The same holds for refinement of the material model with an improper element discretization. Following the multiplicative formulation in the Probabilistic Model Code [17], the modelling uncertainty was defined as the ratio of the experimental to the predicted capacity, $\Theta = R_{\text{exp}}/R_{\text{NLFEA}}$.

3. Solution strategy for NLFEA

All of the choices regarding force equilibrium, kinematic compatibility and constitutive relations influence the modelling uncertainty of NLFEA. Collectively, these choices constitute a strategy for obtaining a solution from NLFEA, or short, a *solution strategy* for NLFEA [2]. For reinforced concrete, the material model for concrete is considered the largest source of modelling uncertainties.

A common way of selecting material models for concrete is to use a uniaxial material model as basis and extend this with additional models that take into account other material effects such as the effects of confinement and lateral cracking. Such an approach can be convenient when the structural effects of different material effects are to be studied, but additional models are normally developed in combination with other complementary models and should not be separated [28]. Alternatively, fully triaxial material models where all material effects are treated, could be used directly. One such fully triaxial material model has been developed by Kotsovos and co-workers since the 1970s and is still subject to improvements [29–38]. In order to make the material model available for practising engineers, it was adapted to a commercial finite element software in the present work. The details are presented in a separate paper [39]. The material model required only one input parameter, the compressive cylinder strength of concrete. A bilinear, elastoplastic model was used for the reinforcement.

Relatively large solid 8-noded finite elements were used for the concrete and the reinforcement was represented by fully

bonded embedded reinforcement elements. Due to the size of the concrete elements, the length of the reinforcement elements corresponding to one integration point was typically in the order of magnitude of the expected crack spacing, and the assumption of perfect bond was thus justified. It should be noted that this is a valid approach specially for NLFEA with large finite elements, where the ultimate limit capacity is sought assuming properly anchored reinforcement. If, on the other hand, the crack pattern at the serviceability limit state is to be studied, a more detailed description of the interface between concrete and reinforcement steel and thus a finer finite element mesh might be needed. Modified Newton-Raphson in combination with line search was used for the iterative solution of the equilibrium equations. A convergence criterion given by $\|\mathbf{R}_{\text{res}}\|/\|\mathbf{R}_{\text{ext}}\| < 0.01$ was used for the equilibrium iterations. $\mathbf{R}_{\text{res}}$ is the vector of nodal residual forces, $\mathbf{R}_{\text{ext}}$ is the vector of nodal external loads and $\|\cdot\|$ indicates that the L_2-norm was used. The loads were applied with constant increment, so that the experimental capacity was reached in 30 load steps.

The solution strategy is discussed in detail in a separate paper, where verification is performed by comparing solutions with different element discretizations, load step sizes and iterative solution procedures [39]. The results show insignificant sensitivity to finite element size and load step size. Validation was performed by comparison of experimental results and results from NLFEA, and the results are presented in the present paper.

4. Characterization of the failure mode

The classical way of characterizing the failure mode of a concrete structure both experimentally and numerically is a matter of subjective judgement. By assessing crack patterns and stress and strain fields at the ultimate limit load, the failure mode can be described as e.g. *diagonal tension*, *shear compression* or *flexure-compression* [40]. Such distinctions are convenient in classical sectional design methods, but have limited applicability to global resistance assessments of large concrete structures where the failure mode could be due to interaction between different sectional forces. For this reason, a more objective characterization to be used in numerical assessments of the failure mode was proposed in the present work.

When a reinforced concrete structure is loaded, cracking of concrete will be initiated at some load level. Upon cracking, the internal forces need to be redistributed. Such redistribution can be associated with the plastic dissipation, i.e. the absorbed non-recoverable strain energy, in the system. If the load is further increased, cracking can either propagate and stabilize if sufficient reinforcement is provided, or propagate progressively to failure. Eventually, also cracking of the sufficiently reinforced structure will propagate to failure when the global redistribution capacity of the reinforcement is exhausted. Hence, reinforcement provides ductility to the brittle concrete by controlling crack propagation and providing sufficient capacity for redistribution of internal forces. This statement was formulated mathematically according to the following expression, where $W_{\text{pl,tot}}$ and $W_{\text{pl,steel}}$ are the plastic dissipation of the system and the reinforcement at failure respectively:

$$X_{\text{ductility}} = \frac{W_{\text{pl,steel}}}{W_{\text{pl,tot}}} \tag{1}$$

The *ductility index*, $X_{\text{ductility}}$, takes values between 0 and 1, and indicates to which degree the failure mode is governed by the reinforcement, and thus the degree of ductility of the failure mode.

5. Statistical inference

According to the definition in the Probabilistic Model Code [17] the modelling uncertainty of benchmark analysis i was defined as the ratio of the experimental to the predicted capacity $\theta_i = R_{\text{exp},i}/R_{\text{NLFEA},i}$. In order to incorporate the modelling uncertainty in a probabilistic analysis, we need to decide the type and parameters of the probability distribution by statistical inference.

5.1. Bayesian data analysis

In Bayesian data analysis both the variable to be modelled and the parameters of the distribution are treated as unknown random variables. The method allows for incorporation of both prior knowledge and observed data, and the statistical uncertainty of the parameters can be estimated from the respective probability distributions. Demonstrations of use can be found in the literature [15, 41, 42] and a thorough treatment of the technique can be found in the work by Gelman et al. [43]. Although not all of the information provided in this section was used in the rest of the paper, it was included for completeness. All the resulting expressions in this section are valid for normally distributed random variables and were adapted from Gelman et al. [43].

The probability distribution of a normally distributed random variable y is fully described as soon as the mean μ and the variance σ^2 is known. According to Bayes' theorem, the conditional distribution of the mean and variance given a set of n observations y_i collected in the array $\mathbf{y}$ can be expressed as:

$$\mathrm{P}(\mu, \sigma^2|\mathbf{y}) \propto \mathrm{P}(\mu, \sigma^2)\,\mathrm{P}(\mathbf{y}|\mu, \sigma^2) \tag{2}$$

$\mathrm{P}(\mu, \sigma^2|\mathbf{y})$ is called the *joint posterior distribution* of μ and σ^2 given the observations $\mathbf{y}$. The posterior distribution of μ and σ^2 is thus proportional to the product of the *prior distribution* $\mathrm{P}(\mu, \sigma^2)$ and the *likelihood* $\mathrm{P}(\mathbf{y}|\mu, \sigma^2)$. Any known information about the random variable, both qualitative and quantitative can be included in the prior distribution.

Having established the joint posterior distribution $\mathrm{P}(\mu, \sigma^2|\mathbf{y})$, a natural extension is to establish the posterior predictive distribution $\mathrm{P}(\tilde{y}|\mathbf{y})$ where $\tilde{y}$ is a future prediction of the outcome of the variable y. In section 5.2 and 5.3 estimates for μ and σ^2, and posterior predictions of $\tilde{y}$ are given for two different prior distributions.

For non-normally distributed random variables, only a limited selection of analytical solutions, the so-called conjugate priors, exist for some distributions, e.g. Poisson or gamma distributions. If these solutions do not exist, the joint posterior and the posterior predictive distributions should be approximated by e.g. numerical integration methods such as Markov Chain Monte Carlo simulation methods or deterministic quadrature rules [43].

5.2. Inference using a non-informative prior distribution

If no information is given about the variable, a non-informative prior distribution can be assumed. An important property of a non-informative prior distribution is that it should be objective, and thus not influence the posterior distribution in any direction. Based on the marginal posterior distributions the expected values and the variances for the mean and the variance are given by (3) to (6), where $\bar{y} = \frac{1}{n}\sum_{i=1}^{n} y_i$ is the sample mean and $s^2 = \frac{1}{n-1}\sum_{i=1}^{n}(y_i - \bar{y})^2$ is the sample variance. Note how the statistical uncertainty, i.e. $\mathrm{Var}[\mu|\mathbf{y}]$ and $\mathrm{Var}[\sigma^2|\mathbf{y}]$, decrease as the number of observations increase.

$$\mathrm{E}[\mu|\mathbf{y}] = \bar{y} \tag{3}$$

$$\mathrm{Var}[\mu|\mathbf{y}] = \frac{n-1}{n-3}\frac{s^2}{n} \tag{4}$$

$$\mathrm{E}[\sigma^2|\mathbf{y}] = \frac{n-1}{n-3}s^2 \tag{5}$$

$$\mathrm{Var}[\sigma^2|\mathbf{y}] = \frac{2(n-1)^2}{(n-3)^2(n-5)}s^4 \tag{6}$$

It can be shown that the posterior prediction $\tilde{y}$ can be modelled as a t-distributed random variable with location $\bar{y}$, scale $s^2(1 + 1/n)$ and $n - 1$ degrees of freedom. A future observation can thus be modelled by (7) where $t_{\mathrm{n\text{-}1}}$ is a centrally t-distributed random variable with $n - 1$ degrees of freedom. For large n the t-distribution approaches the normal distribution.

$$\tilde{y} = \bar{y} + t_{\mathrm{n\text{-}1}}\, s\sqrt{1 + \frac{1}{n}} \tag{7}$$

5.3. Inference using a conjugate prior distribution

If prior information exists, this can be included in the prior distribution. One technique that ensures closed form solutions is to select a joint prior distribution of the same form as the

likelihood. This is called a *conjugate prior distribution*. The parameters of the resulting posterior distribution are given in (8) to (11), where n_0 is the number of samples that forms the basis of the prior knowledge and $\nu_0 = n_0 - 1$ is the prior number of degrees of freedom.

$$\mu_\mathrm{n} = \frac{n_0\mu_0 + n\bar{y}}{n_0 + n} \tag{8}$$

$$n_\mathrm{n} = n_0 + n \tag{9}$$

$$\nu_\mathrm{n} = \nu_0 + n = n_0 + n - 1 \tag{10}$$

$$\nu_\mathrm{n}\sigma_\mathrm{n}^2 = \nu_0\sigma_0^2 + (n-1)s^2 + \frac{n_0 n}{n_0 + n}(\bar{y} - \mu_0)^2 \tag{11}$$

The expected values and variances are given in (12) to (15). Notice how (12) and (14) approach (3) and (5) if no prior information exists.

$$\mathrm{E}[\mu|\mathbf{y}] = \mu_\mathrm{n} \tag{12}$$

$$\mathrm{Var}[\mu|\mathbf{y}] = \frac{\nu_\mathrm{n}}{\nu_\mathrm{n} - 2}\frac{\sigma_\mathrm{n}^2}{n_\mathrm{n}} \tag{13}$$

$$\mathrm{E}[\sigma^2|\mathbf{y}] = \frac{\nu_\mathrm{n}}{\nu_\mathrm{n} - 2}\sigma_n^2 \tag{14}$$

$$\mathrm{Var}[\sigma^2|\mathbf{y}] = \frac{2\nu_\mathrm{n}^2}{(\nu_\mathrm{n} - 2)^2(\nu_\mathrm{n} - 4)}\sigma_\mathrm{n}^4 \tag{15}$$

It can be shown that the posterior prediction $\tilde{y}$ can be modelled as a t-distributed random variable with location μ_n, scale $\sigma_\mathrm{n}^2(1 + 1/n_\mathrm{n})$ and ν_n degrees of freedom. A future observation can thus be modelled by (16) where t_{ν_n} is a centrally t-distributed random variable with ν_n degrees of freedom.

$$\tilde{y} = \mu_\mathrm{n} + t_{\nu_\mathrm{n}}\sigma_\mathrm{n}\sqrt{1 + \frac{1}{n_\mathrm{n}}} \tag{16}$$

5.4. The probability distribution of the modelling uncertainty

The probability distribution of the modelling uncertainty is generally not known in advance, however, it is suggested to represent it as a log-normally distributed random variable [17]. The relation between the parameters of a log-normal distribution μ_ln and σ_ln and the mean and variance of the variable itself are given in (17) and (18), where $V = \sigma/\mu$ is the coefficient of variation.

$$\mu_\mathrm{ln} = \ln\mu - \frac{1}{2}\ln(V^2 + 1) \tag{17}$$

$$\sigma_\mathrm{ln} = \sqrt{\ln(V^2 + 1)} \tag{18}$$

In order to perform Bayesian inference on a normally distributed random variable, each observation of the modelling uncertainty θ_i is assigned to y_i. If, on the other hand, the random variable is log-normally distributed, the natural logarithm of each observation $\ln\theta_i$ is assigned to y_i. In order to verify the selected distribution type, the Shapiro-Wilk test for normality [44] with the improvements proposed by Royston [45] was applied. A test statistic was calculated and used as input for a hypothesis test where the null-hypothesis stated that the sample was normally distributed. The P-value was calculated and compared to a 5% level of significance.

6. Quantification of the modelling uncertainty

The global results from 38 benchmark analyses are summarized in Table 1 and Figure 2. The sample consisted of seven short and five slender walls by Lefas et al. [24], one beam by Kotsovos [20], 12 beams by Bresler and Scordelis [40], two frames by Ernst et al. [46], two frames by Vecchio and Balopoulou [47] and Vecchio and Emara [48], one deep beam by Cervenka and Gerstle [49] and eight beams by Jelic et al. [50]. All of the references reported the nominal geometries, and the cylinder strength of the concrete and the yield strength of the reinforcement steel based on a number of material samples. The cylinder strength was used directly as the only input material parameter for the concrete material model, and was

not calibrated in order to improve the results in any of the analyses. It was assumed that the concrete within one structural component, i.e. one beam, frame or wall, originated from one batch, and that the reported cylinder strength was measured on samples from the same batch. No information about the spatial variability of the strength was reported, and was thus not considered in the analyses.

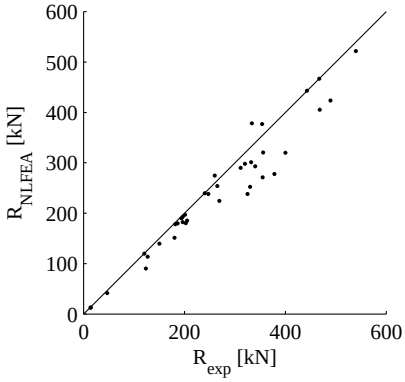

Figure 2: Experimental capacity and predicted capacity for the 38 benchmark analyses.

Most model predictions were slightly underestimating the experimental capacity, denoted by $\theta_i > 1.0$, and the variation was small. The results from the Shapiro-Wilk test on either $y_i = \theta_i$ or $y_i = \ln \theta_i$, i.e. testing for either normality or log-normality, are summarized in Table 2, where the P-value was compared to a 5% level of significance. The test did not reject that Θ could be represented as a log-normally distributed random variable. The results were confirmed by the probability plots in Figure 3 where the scatter plot is slightly more concentrated along the straight line for the log-normal distribution than for the normal distribution. Note that the straight lines are indicative only, as they are based on the sample mean and sample variance.

Based on these results, Bayesian inference with a non-informative prior was performed on the sample $\mathbf{y}$ where $y_i = \ln \theta_i$. The expressions in section 5.2 resulted in $\mu_{\ln\Theta} = 0.092$ and $\sigma_{\ln\Theta} = 0.108$, and by using the expressions in section 5.4 a mean $\mu_\Theta = 1.10$, a standard deviation $\sigma_\Theta = 0.12$ and a coefficient of variation $V_\Theta = 10.9\%$ was calculated.

Figure 4a shows the modelling uncertainty plotted against the cylinder strength. No simple linear trend can be observed, and the resulting linear correlation coefficient was 0.013 which confirms that observation. It might be interesting also to check the correlation to other input parameters, but as the sample contained benchmark experiments with varying reinforcement layouts and structural forms, no parameters except the cylinder strength were directly comparable. Figure 4b shows the modelling uncertainty plotted against the ductility index, as defined in section 4, for all the benchmark analyses. Depending on the ductility index, the observations might be grouped in two separate domains: one brittle and one ductile.

7. Discussion

The level of detail which is needed for the material model depends on the phenomena that are to be studied in the analysis. In the present study, the ultimate limit capacity was sought, and for this application the simple fully triaxial material model [29, 30] was appropriate. The results were supporting the conclusions from Engen et al. [2] advising a shift of the attention from a detailed description of the post-cracking tensile behaviour to a rational description of the pre-cracking compressive behaviour of concrete in analyses where large finite elements are used. Despite the simple form of the material model and the coarse meshes of linear solid elements, the resulting modelling uncertainty had a low standard deviation, and the mean value close to one indicated a small model bias.

A new method for characterization of the failure mode was presented. The method characterized the failure mode in terms of the ductility index, $X_{\text{ductility}}$, defined as the ratio between the plastic dissipation of the reinforcement and the total plastic dissipation of the system. It was regarded as an advantage of the method that it was objective and unambiguous compared to traditional characterizations based on subjective judgement. This seemed to be particularly relevant for failure modes where the interaction between several sectional forces was governing. The objective characterization should be complemented by a

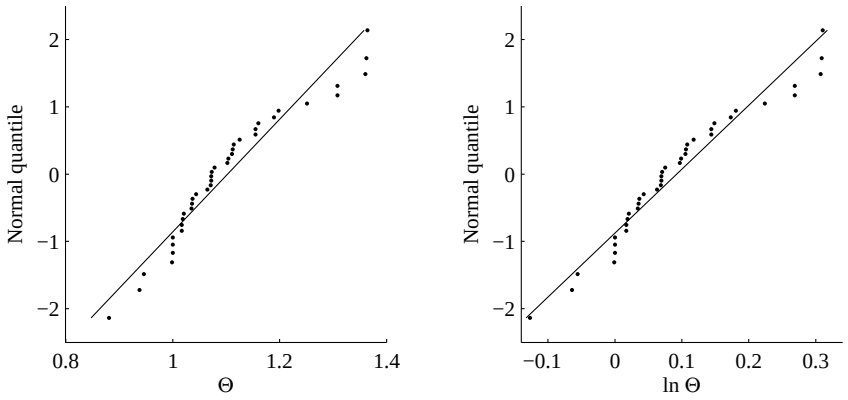

(a) Normal distribution. (b) Log-normal distribution.

Figure 3: Probability plot for the modelling uncertainty Θ assuming a) normal and b) log-normal distribution.

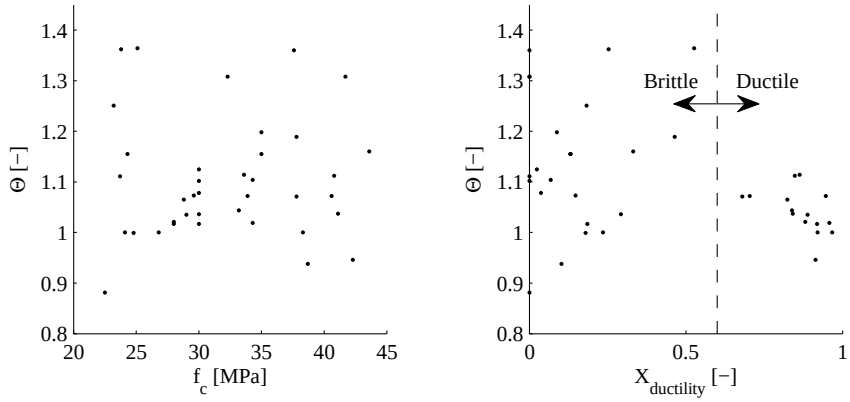

(a) Cylinder strength. (b) Ductility index.

Figure 4: Correlation between modelling uncertainty Θ and a) cylinder strength f_c and b) ductility index $X_{\text{ductility}} = W_{\text{pl,steel}}/W_{\text{pl,tot}}$.

description of the failure mode, e.g. in terms of the crack pattern, stress and strain contours and displacements.

If all the redistribution, i.e. the plastic dissipation, is assigned to the concrete, the structure is likely to fail in a brittle manner due to the low redistribution capacity of the concrete. The brittle failure modes governed by the concrete have a higher inherent physical uncertainty and are often more difficult to predict with a high accuracy compared to the ductile counterpart of failure modes governed by the reinforcement. The sources for the high inherent uncertainty of the brittle failure modes are the spatial variability and the mean and standard deviation of the material properties within the concrete batch, and the correlation between the cylinder strength and other parameters of the concrete as described in Section 2. Because these variations were not controlled in the uncerlying experiments, they were not considered explicitly in the analyses, thus they were implicitly included in the modelling uncertainty. The modelling uncertainty of the ductile failure modes, on the other hand, would have a lower contribution from physical uncertainties due to the lower physical uncertainties inherent to the reinforcement steel. This statement serves as a rational explanation to the results from earlier studies of the modelling uncertainty in connection to prediction of the capacity of reinforced concrete [3, 19]. As an indication on the dependency of Θ on the failure mode, the benchmark analyses could be separated in two domains, e.g. a brittle domain for $X_{\text{ductility}} < 0.6$ and a ductile domain for

$X_{\text{ductility}} \geq 0.6$, as shown in Figure 4b. Bayesian inference resulted in $\mu_\Theta = 1.14$ and $\sigma_\Theta = 0.14$, and $\mu_\Theta = 1.04$ and $\sigma_\Theta = 0.05$, for the brittle and ductile domain respectively, and the standard deviation of the modelling uncertainty thus got its largest contribution from the brittle domain.

Based on the discussion above, the separation of uncertainties such that a pure modelling uncertainty is obtained is not straight forward and it is reasonable to keep the present definition and note that the estimated modelling uncertainty also includes contributions from the physical uncertainties. With the present definition of the modelling uncertainty, and treating the physical uncertainties on hierarchical levels, the only contribution to the physical uncertainties that should be included in a reliability assessment are those related to the variability of the material supply between different producers. However, reasonable assumptions for the quantification of this variability is beyond the scope of this paper and calls for further research.

If the capacity of a ductile experiment was underestimated, the calculated ductility index would also be underestimated, resulting in a low $x_{\text{ductility},i}$, a low predicted capacity and a high θ_i. This represented a slight weakness of the characterization of the failure mode presented in the present paper. It should be noted that the underestimation could be both due to solving the wrong equations, i.e. inadequate material modelling or geometric idealization, or due to wrong solution of the equations, i.e. inadequate finite element discretization or iterative solution of the non-linear equilibrium equations. On the other hand, if the capacity of a brittle experiment was properly estimated, this resulted in a low $x_{\text{ductility},i}$ and $\theta_i \approx 1.0$, and a high $x_{\text{ductility},i}$ would in all cases indicate that the failure mode is indeed ductile.

In order to perform all the benchmark analyses in a consistent manner, the external load was applied with constant load increments such that the experimental capacity was reached in 30 load steps. This was the main reason for several of the points in Figure 4a and 4b being horizontally aligned. Due to the discretized load application, a higher load could in principle be reached if the load was continuously increased to failure. If several benchmark analyses in reality could have yielded higher capacities, this would influence the estimated parameters of the modelling uncertainty. A resulting theoretical deviation was found to be in the order of magnitude of the statistical uncertainty of the estimated parameters, and was thus not studied further in detail.

Ditlevsen and Madsen [51] note that whatever degree of refinement of the mechanical model, some modelling uncertainty will remain, and at some degree of refinement, the physical and statistical uncertainty will dominate the total uncertainty of the problem. This indicates that a reasonable target for the modelling uncertainty could be in the order of the dominating physical or statistical uncertainty. In the recommendations published by *fib* [52] it is stated that the coefficient of variation of the modelling uncertainty should be less than 30%. Assuming a target reliability level including sensitivity factors, the global safety factor for modelling uncertainty used in Model Code 2010 corresponds to a coefficient of variation of 5-15% depending on the assumed bias [5]. The coefficient of variation obtained in the present study was thus considered adequate. It should be noted that the resulting modelling uncertainty reported in the present paper is related to one specific solution strategy, i.e. one specific set of choices regarding force equilibrium, kinematic compatibility and constitutive relations. A change of solution strategy is expected to result in different parameters for the modelling uncertainty that need to be quantified.

The modelling uncertainty as treated in the present project can be incorporated in reliability assessments in several ways. In semi-probabilistic methods, the coefficient of variation can be included in the calculation of the total coefficient of variation following the approach suggested by Schlune et al. [3] or as a separate reduction factor as discussed by e.g. Kadlec and Cervenka [53]. Θ could be incorporated directly as a basic variable in a procedure based on e.g. a response surface and a first order reliability method as demonstrated by Belletti et al. [12]. In a full probabilistic method, Θ can be simulated by drawing random samples from a normal, log-normal or a t-distribution depending on which distribution is the most suitable.

8. Conclusions

Results from a range of benchmark analyses where a fully triaxial material model for concrete and relatively large solid elements were used, showed that the modelling uncertainty could be represented as a log-normally distributed random variable with a mean 1.10 and a standard deviation of 0.12. These results indicate that the global safety factor for modelling uncertainty suggested in Model Code 2010 for numerical models subjected to a high level of validation is valid. The new method for characterizing the failure mode that was developed was successfully applied, and the results indicated that the physical uncertainties influence the estimated parameters of the modelling uncertainty. Because the physical uncertainties related to variation of the concrete compressive strength within and between batches from one producer were not explicitly considered in the NLFEA in the present study, these uncertainties were implicitly included in the estimated modelling uncertainty. With the present definition of the modelling uncertainty, only the physical uncertainties related to the variability of the material supply between different producers should thus be included in a reliability assessment. It is worth noting that all the cases that were studied, relate to laboratory experiments with more or less well-defined boundary and loading conditions. In a real concrete structure, the physical uncertainties might increase e.g. due to inadequate curing conditions or variable quality of workmanship, and the modelling uncertainty might increase due to e.g. idealization of geometry, load application and boundary conditions. In the further work, different possibilities for including the modelling uncertainty in a reliability assessment will be studied. This is considered crucial for obtaining realistic estimates of the design load carrying capacity or the reliability of both new and existing concrete structures.

Acknowledgments

The work presented in this paper is part of an industrial PhD funded by Multiconsult ASA and The Research Council of Norway. Morten Engen would like to thank his supervisors and all colleagues in the Marine Structures Department at Multiconsult for valuable discussions and particularly *Per Horn*, former Senior Vice President of Multiconsult, for having the courage to initiate the research project.

References

[1] D.-E. Brekke, E. Åldstedt, H. Grosch, Design of Offshore Concrete Structures Based on Postprocessing of Results from Finite Element Analysis (FEA): Methods, Limitations and Accuracy, in: Proceedings of the Fourth (1994) International Offshore and Polar Engineering Conference, 1994.

[2] M. Engen, M. A. N. Hendriks, J. A. Øverli, E. Åldstedt, Solution strategy for non-linear Finite Element Analyses of large reinforced concrete structures, Structural Concrete, 16(3), 2015, 389–397.

[3] H. Schlune, M. Plos, K. Gylltoft, Safety formats for non-linear analysis of concrete structures, Magazine of Concrete Research, 64(7), 2012, 563–574.

[4] V. Cervenka, Reliability-based non-linear analysis according to *fib* Model Code 2010, Structural Concrete, 14(1), 2013, 19–28.

[5] *fib*, *fib* Model Code for Concrete Structures 2010, Ernst & Sohn, 2013.

[6] B. Belletti, C. Damoni, M. A. Hendriks, Development of guidelines for nonlinear finite element analyses of existing reinforced and pre-stressed beams, European Journal of Environmental and Civil Engineering, 15(9), 2011, 1361–1384.

[7] H. Schlune, M. Plos, K. Gylltoft, Safety formats for nonlinear analysis tested on concrete beams subjected to shear forces and bending moments, Engineering Structures, 33(8), 2011, 2350–2356.

[8] D. L. Allaix, V. I. Carbone, G. Mancini, Global safety format for nonlinear analysis of reinforced concrete structures, Structural Concrete, 14(1), 2013, 29–42.

[9] B. Belletti, C. Damoni, J. A. den Uijl, M. A. N. Hendriks, J. Walraven, Shear resistance evaluation of prestressed concrete bridge beams: *fib* Model Code 2010 guidelines for level IV approximations, Structural Concrete, 14(3), 2013, 242–249.

[10] B. Belletti, C. Damoni, M. A. Hendriks, J. A. den Uijl, Nonlinear finite element analyses of reinforced concrete slabs: Comparison of safety formats, in: FraMCoS-8, 2013.

[11] B. Belletti, C. Damoni, M. A. N. Hendriks, A. de Boer, Analytical and numerical evaluation of the design shear resistance of reinforced concrete slabs, Structural Concrete, 15(3), 2014, 317–330.

[12] B. Belletti, M. Pimentel, M. Scolari, J. C. Walraven, Safety assessment of punching shear failure according to the level of approximation approach, Structural Concrete, 16(3), 2015, 366–380.

[13] M. Pimentel, E. Brühwiler, J. A. Figueiras, Safety examination of existing concrete structures using the global resistance safety factor concept, Engineering Structures, 70, 2014, 130–143.

[14] M. Blomfors, M. Engen, M. Plos, Evaluation of safety formats for non-linear Finite Element Analyses of statically indeterminate concrete structures subjected to different load paths, Structural Concrete, 17(1), 2016, 44–51.

[15] R. Zhang, S. Mahadevan, Model uncertainty and Bayesian updating in reliability-based inspection, Structural Safety, 22(2), 2000, 145–160.

[16] R. Rackwitz, Predictive distribution of strength under control, Materials and Structures, 16(4), 1983, 259–267.

[17] JCSS, Probabilistic Model Code, 12th draft, Joint Committee on Structural Safety, 2001.

[18] M. A. Rashid, M. A. Mansur, P. Paramasivam, Correlations between Mechanical Properties of High-Strength Concrete, Journal of Materials in Civil Engineering, 14(3), 2002, 230–238.

[19] B. Ellingwood, T. V. Galambos, Probability-based criteria for structural design, Structural Safety, 1(1), 1982, 15–26.

[20] M. D. Kotsovos, A fundamental explanation of the behaviour of reinforced concrete beams in flexure based on the properties of concrete under multiaxial stress, Materials and Structures, 15(90), 1982, 529–537.

[21] G. M. Kotsovos, Assessment of the flexural capacity of RC beam/column elements allowing for 3d effects, Engineering Structures, 33, 2011, 2772–2780.

[22] G. M. Kotsovos, D. M. Cotsovos, M. D. Kotsovos, A. N. Kounadis, Seismic behaviour of RC walls: an attempt to reduce reinforcement congestion, Magazine of Concrete Research, 63(4), 2011, 235–246.

[23] G. M. Kotsovos, Seismic design of RC beam-column structural elements, Magazine of Concrete Research, 63(7), 2011, 527–537.

[24] I. D. Lefas, M. D. Kotsovos, N. N. Ambraseys, Behaviour of Reinforced Concrete Structural Walls: Strength, Deformation Characteristics, and Failure Mechanism, ACI Structural Journal, 87(1), 1990, 23–31.

[25] K.-H. Reineck, D. Kuchma, K. S. Kim, S. Marx, Shear Database for Reinforced Concrete Members without Shear Reinforcement, ACI Structural Journal, 100(2), 2003, 240–249.

[26] O. Ditlevsen, Model uncertainty in structural reliability, Structural Safety, 1(1), 1982, 73–86.

[27] P. J. Roache, Verification of Codes and Calculations, AIAA Journal, 36(5), 1998, 696–702.

[28] F. J. Vecchio, Non-linear finite element analysis of reinforced concrete: at the crossroads?, Structural Concrete, 2(4), 2001, 201–212.

[29] M. D. Kotsovos, A mathematical description of the strength properties of concrete under generalized stress, Magazine of Concrete Research, 31(108), 1979, 151–158.

[30] M. D. Kotsovos, A mathematical model of the deformational behavior of concrete under generalised stress based on fundamental material properties, Materials and Structures, 13(76), 1980, 289–298.

[31] C. Bédard, M. D. Kotsovos, Application of NLFEA to Concrete Structures, Journal of Structural Engineering, 111(12), 1985, 2691–2707.

[32] F. González Vidosa, M. D. Kotsovos, M. N. Pavlovic, Three-dimensional non-linear finite-element model for structural concrete. Part 1: main features and objectivity study, Proceedings of the ICE - Structures and Buildings, 91, 1991, 517–544.

[33] F. González Vidosa, M. D. Kotsovos, M. N. Pavlovic, Three-dimensional non-linear finite-element model for structural concrete. Part 2: generality study, Proceedings of the ICE - Structures and Buildings, 91, 1991, 545–560.

[34] M. D. Kotsovos, M. N. Pavlovic, Structural Concrete: Finite-element analysis for limit-state design, Thomas Telford, 1995.

[35] M. D. Kotsovos, K. V. Spiliopoulos, Modelling of crack closure for finite-element analysis of structural concrete, Computers & Structures, 69(3), 1998, 383–398.

[36] D. M. Cotsovos, M. N. Pavlovic, Simplified FE model for RC structures under earthquakes, Proceedings of the ICE - Structures and Buildings, 159(SB2), 2006, 87–102.

[37] K. V. Spiliopoulos, G. C. Lykidis, An efficient three-dimensional solid finite element dynamic analysis of reinforced concrete structures, Earthquake Engineering and Structural Dynamics, 35(2), 2006, 137–157.

[38] G. Markou, M. Papadrakakis, Computationally efficient 3D finite element modeling of RC structures, Computers and Concrete, 12(4), 2013, 443–498.

[39] M. Engen, M. A. N. Hendriks, J. A. Øverli, E. Åldstedt, Material Model for Non-linear Finite Element Analyses of Large Concrete Structures, Submitted for review, 2016.

[40] B. Bresler, A. C. Scordelis, Shear Strength of Reinforced Concrete Beams, Journal of the American Concrete Institute, 60(1), 1963, 51–74.

[41] E. L. Droguett, A. Mosleh, Bayesian Methodology for Model Uncertainty Using Model Performance Data, Risk Analysis, 28(5), 2008, 1457–1476.

[42] D. L. Allaix, V. I. Carbone, G. Mancini, Modelling uncertainties for the loadbearing capacity of corroded simply supported RC beams, Structural Concrete, 16(3), 2015, 333–341.

[43] A. Gelman, J. B. Carlin, H. S. Stern, D. B. Dunson, A. Vehtari, D. B. Rubin, Bayesian Data Analysis, CRC Press, 3 edn., 2014.

[44] S. S. Shapiro, M. B. Wilk, An analysis of variance test for normality (complete samples), Biometrika, 52(3 and 4), 1965, 591–611.

[45] P. Royston, Approximating the Shapiro-Wilk W-test for non-normality, Statistics and Computing, 2(3), 1992, 117–119.

[46] G. C. Ernst, G. M. Smith, A. R. Riveland, D. N. Pierce, Basic Reinforced Concrete Frame Performance Under Vertical and Lateral Loads, ACI Journal, 70(4), 1973, 261–269.

[47] F. J. Vecchio, S. Balopoulou, On the Nonlinear Behaviour of Reinforced Concrete Frames, Canadian Journal of Civil Engineering, 17(5), 1990, 698–704.

[48] F. J. Vecchio, M. B. Emara, Shear Deformations in Reinforced Concrete Frames, ACI Structural Journal, 89(1), 1992, 46–56.

[49] V. Cervenka, K. H. Gerstle, Inelastic Analysis of Reinforced Concrete Panels: Experimental Verification and Application, IABSE Publications, 32, 1972, 31–45.

[50] I. Jelic, M. N. Pavlovic, M. D. Kotsovos, Performance of structural-

concrete members under sequential loading and exhibiting points of inflection, Computers and Concrete, 1(1), 2004, 99–113.

[51] O. Ditlevsen, H. O. Madsen, Structural Reliability Methods, Coastal, Maritime and Structural Engineering, Department for Mechanical Engineering, Technical University of Denmark, internet edition 2.2.5 edn., 2005.

[52] *fib*, Bulletin 45: Practitioner's guide to finite element modelling of reinforced concrete structures, International Federation for Structural Concrete (*fib*), 2008.

[53] L. Kadlec, V. Cervenka, Uncertainty of numerical models for punching resistance of rc slabs, in: Concrete - Innovation and Design, *fib* Symposium, Copenhagen May 18-20, 2015.

Table 1: Summary of the results from the benchmark analyses. f_c is the cylinder strength in MPa, $R_{\text{exp},i}$ and $R_{\text{NLFEA},i}$ are the experimental and predicted capacities in kN, θ_i is the modelling uncertainty and $x_{\text{ductility},i} = W_{\text{pl,steel}}/W_{\text{pl,tot}}$ is the ductility index given by the ratio of the plastic dissipation of the reinforcement and the total plastic dissipation.

Ref.	**Experiment**	f_c	$R_{\text{exp},i}$	$R_{\text{NLFEA},i}$	θ_i	$x_{\text{ductility},i}$
[24]	SW11	42.3	260.00	274.94	0.95	0.914
	SW12	43.6	340.00	293.20	1.16	0.331
	SW13	32.3	330.00	252.35	1.31	0.000
	SW14	33.2	265.00	253.92	1.04	0.839
	SW15	33.9	320.00	298.39	1.07	0.946
	SW16	41.7	355.00	271.46	1.31	0.000
	SW17	41.1	247.00	238.22	1.04	0.841
	SW21	33.6	127.00	113.99	1.11	0.863
	SW22	40.6	150.00	139.94	1.07	0.704
	SW23	37.8	180.00	151.38	1.19	0.464
	SW24	38.3	120.00	120.01	1.00	0.920
	SW26	25.1	123.00	90.20	1.36	0.526
[20]	B1	37.8	13.60	12.69	1.07	0.680
[40]	OA-1	22.5	333.60	378.53	0.88	0.000
	OA-2	23.7	355.84	320.40	1.11	0.000
	OA-3	37.6	378.08	277.93	1.36	0.000
	A-1	24.1	467.04	466.96	1.00	0.235
	A-2	24.3	489.28	423.80	1.15	0.132
	A-3	35.0	468.37	405.60	1.15	0.130
	B-1	24.8	442.58	443.00	1.00	0.179
	B-2	23.2	400.32	320.00	1.25	0.183
	B-3	38.7	353.62	377.17	0.94	0.103
	C-1	29.6	311.36	290.27	1.07	0.147
	C-2	23.8	324.70	238.33	1.36	0.253
	C-3	35.0	269.10	224.72	1.20	0.088
[46]	2D18	40.8	46.40	41.72	1.11	0.848
	2D18H	28.8	14.10	13.24	1.07	0.824
[47]	BF1	29.0	540.00	521.98	1.03	0.888
[48]	BF2	30.0	332.00	301.31	1.10	0.000
[49]	W2	26.8	240.00	240.00	1.00	0.967
[50]	HDCB3	30.0	202.70	180.16	1.13	0.024
	HDCB4	30.0	196.50	182.29	1.08	0.037
	MDCB3	28.0	193.90	189.98	1.02	0.881
	MDCB4	28.0	196.40	193.14	1.02	0.919
	LDCB3	30.0	181.60	178.54	1.02	0.185
	LDCB4	30.0	186.20	179.70	1.04	0.292
	G21	34.3	204.80	185.53	1.10	0.069
	G22	34.3	200.80	197.01	1.02	0.958

Table 2: Summary of results from the Shapiro-Wilk test for normality of Θ. W is the Shapiro-Wilk test statistic and the P-value is the probability of making the current observation given that the observations are normally distributed.

$\mathbf{y_i}$	**W**	***P*-value**	
θ_i	0.9232	$0.012 < 0.05$	$\Rightarrow$ Reject
$\ln \theta_i$	0.9461	$0.066 > 0.05$	$\Rightarrow$ Do not reject